

# Transmission Lines Fault Location Based on High-Frequency Components Technique: a general formulation for estimation of the dominant frequency

L. U. Iurinic, R. G. Ferraz, E. S. Guimarães, A. S. Bretas

**Abstract**— This work shows an analytical approach to relate the frequency spectrum of transient voltage generated by faults with fault location. An equation of the spectrum produced by travelling wave phenomenon is developed and is used to generate a fault location equation. The equation relates a characteristic frequency of signal with system parameters and fault distance. In order to demonstrate the effectiveness of the developed equations, most general faults are simulated using different values for equivalent impedance. Results show a very good accuracy in fault location.

**Keywords:** fault location, characteristic frequency, frequency spectrum, travelling waves.

## I. INTRODUCTION

ELECTRIC power lines are components that cover a great surface. Hence they are constantly exposed to faults. Some causes of fault are bad network maneuvers, objects or vegetation being in contact, decline of isolation due lightning or aging, vandalism among others. A fast and accurate fault location technique is essential for restoration of the system as soon as possible.

Most established and known approaches for fault location are based on the apparent impedance equation. It relates voltages and current phasors with line impedance and unknown distance to the fault, fault resistance and fault current. Equation is solved for distances depending on the system treated. For transmission lines with feedings in both sides, some established methods are [1]-[2] that deal with current distribution factors. For radial systems with multiple branches and considerable shunt admittance, a generalized

equation is developed in [3], where two second order polynomials for fault distance are developed.

Another concept for fault location is the travelling wave method. This approach is treated in early works like [4] and is based in a simple idea. Due the distributed nature of electric line parameters, a fault produce a voltage and current wave that propagates in two directions of the line. Wave fronts can then be detected in different time instants when they arrive to system terminals. Then, knowing the propagation velocity of wave and time difference among arrivals, it is possible to calculate the fault distance. The advantage of using this approach is a minor influence of fault type and resistance, source parameters, current transformers saturation and load state of the system [5]. Furthermore, apparent impedance methods need information of some fundamental frequency cycles to work. Indeed, travelling wave can work with information of only a fraction of cycle. It leads the possibility of an ultra-high velocity technique.

When information from two terminals is available the problem is relatively easy to solve. Since waves arrive firstly to the nearest terminal, a simple relation between time and velocity can be used to calculate fault distance. In order to detect wave fronts many detection methods have been proposed, like wavelets transform [6], filtering [7] or Park's transformation [8]-[9]. However, to be possible to detect the wave fronts, expensive high frequency measurement devices are required in both ends. Furthermore, time references of devices must be synchronized. This task is actually made by GPS technology.

If only one terminal data are available, time delay between successive wave's reflections must be detected. Nonetheless, for faults involving ground, also reflections from the remote terminal can be observed. Some proposed solution of this problem are presented in [10] and [7]

Dealing with the problematic of detecting and identifying multiples wave's reflections, current or voltage spectrum can be used as a signature for estimating the fault distance. The voltage or current spectrum produced by a short circuit in a line is proportional to its impulsive response [11]. It is composed by a series of peaks in frequencies related with fault location and reflection coefficients. Swift [12] analyzes the natural frequency spectrum generated by faults. He treats this frequency as a noise that affects relays performances and shows that it is inversely proportional to fault distance. On the other hand, the equation presented there is incomplete because

---

The authors gratefully acknowledge Coordenação de Aperfeiçoamento de Pessoal de Nível Superior (CAPES) and Conselho Nacional de Desenvolvimento Científico e Tecnológico (CNPq) for the financial support of this study.

L. U. Iurinic, R. G. Ferraz and A. S. Bretas are with Universidade Federal do Rio Grande do Sul, Av. Osvaldo Aranha 103, Porto Alegre, RS, Brasil (e-mail of corresponding author: uirinic@ece.ufrgs.com.br)

E. S. Guimarães is with Companhia Estadual de Distribuição de Energia Elétrica (CEEE-D), Av. Joaquim Porto Villanova 201, Porto Alegre, Brazil (e-mail: edersong@ceee.com.br)

Paper submitted to the International Conference on Power Systems Transients (IPST2013) in Vancouver, Canada July 18-20, 2013.

only refers to extreme cases of the upstream impedance from Relay.

In [13] a formulation is proposed by implementing a mother wavelet inferred from the own measured signal. However these methods continue with the consideration of extreme values of the upstream impedance from Digital Fault Recorder (DFR).

The aim of this paper is to develop a general formulation for calculating the dominant frequencies due to fault occurrence in transmission lines. Then, to consider the source impedances effect into a simple and practical equation. Reference [14] treats the same problem. On the other hand, the presented paper not only presents an equation for fault location, but also derives a transfer function that gives the entire spectrum due a fault. This transfer function also can be helpful in future works to solve the problem of faulted branch identification. Finally, the formulation is implemented using Matlab® and validated with ATP (Alternative Transient Program) simulations.

## II. THEORETICAL BACKGROUND OF THE CHARACTERISTIC FREQUENCY

Consider the line-to-ground fault in a single-phase transmission line illustrated in Fig.1, where  $Z_c$  is the surge line impedance and  $X_s$  is the equivalent reactance at bus A.

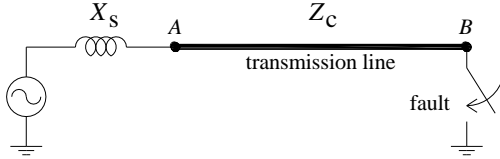


Fig. 1. Faulted single-phase transmission line

For a fault with zero resistance, the voltage at bus B is collapsed to zero by a negative step surge. This wave goes toward bus A in a time  $\tau$ , cancelling out the voltage as it travels. As explained in [12], the surge will be reflected at both ends generating a noise superposed with the source voltage. The dominant noise frequency can be represented as [12]:

$$f_{noise} = \frac{1}{n_p \tau}, \quad (1)$$

Where  $\tau$  is the transit time and  $n_p$  is related to the propagation of the travelling wave along the transmission line. If  $X_s \gg Z_c$ ,  $n_p$  will be very close to 4 and if  $X_s \ll Z_c$ ,  $n_p$  will be close to 2.

According with [13], the dominant noise frequency can be measured and used to isolate  $\tau$  from (1). Since  $\tau$  is directly related with fault distance, the noise frequency is generally referred as characteristic frequency ( $f_c$ ) of high-frequency components of current and voltages generated by faults. This approach requires the knowledge of  $n_p$  that has been assumed as 2 or 4 on prior works. However, for the case where  $X_s$  is neither small nor large,  $f_c$  lies in fact between the two extremes. This distortion was identified in [12] and referred as the interference of the waves with its own multiple reflections and with the ground mode wave and its reflections. To

illustrate what is described above, consider the single-phase transmission line modeled in ATP and shown in Fig. 2.

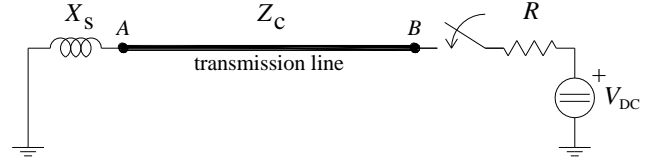


Figure 2. Faulted single-phase transmission line modeled in ATP

The voltage step injected by the fault is simulated by switching a DC source of 1 V in node B. The length of the transmission line is 120 km, the impedance  $Z_c$  is 962  $\Omega$  and the wave propagation time is 400.27  $\mu s$ . Voltage at node A is showed in Fig. 3 for three different  $X_s$  values. Remind that this situation is not real and is only an illustration to show the waves behavior.

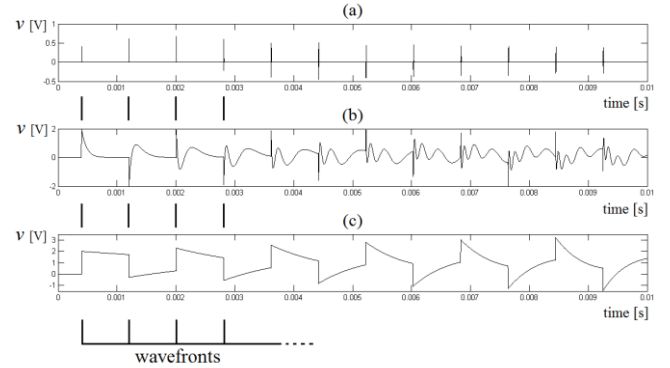


Figure 3. Results of voltage measured at bus A performed with ATP: a)  $X_s = 0.188 \Omega$ ; b)  $X_s = 30.159 \Omega$ ; c)  $X_s = 1884.955 \Omega$  (at 60 Hz)

Cases (a) and (c) are the both extreme conditions for the  $f_c$ , where  $n_p$  is 2 and 4 respectively. In case (b) the reactance at node A have an intermediate value, leading to significant wave interferences. In such case  $n_p$  is equal to 2.38, instead of 2. Note that wave fronts are the same in all cases, showing that (1) must be modified to take into account the value of  $X_s$ .

## III. PROPOSED EQUATIONS FOR CHARACTERISTICS FREQUENCIES

A general formulation for estimation of the characteristic frequency generated by faults occurrence is obtained from a transfer function of a single-phase transmission line. This formulation can be used for fault location in transmission lines based on high-frequency components technique.

### A. Equation of spectrum

The problem identified in the previous section can be solved using the Lattice diagram shown in Fig. 4. Waves will be reflected and transmitted at bus 1 and 2 according to the product of travelling waves with reflection and transmission coefficients ( $h_r$  and  $h_t$  respectively). If these coefficients are frequency dependent, the reflected and transmitted waves are convolutions in time with the coefficients. Therefore, in frequency domain the operations are simple products. This

suggests that  $h_r$  and  $h_t$  are the impulse responses of linear systems with incident waves as input and reflected and transmitted waves as outputs.

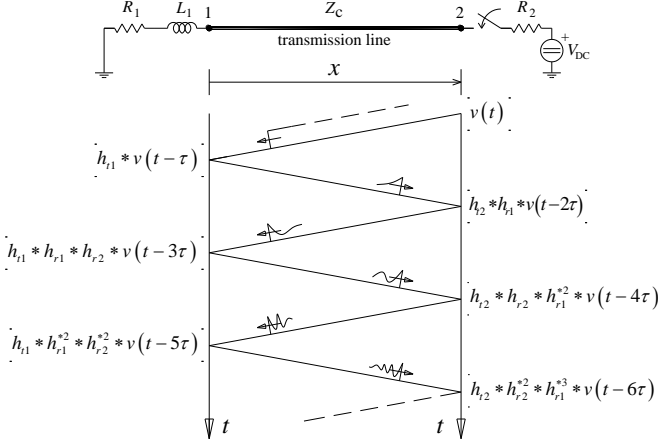


Fig. 4. Lattice diagram of a single-phase transmission line

The measured voltage at end one is composed by a sum of transmitted voltage waves given by:

$$v_1(t) = h_{r1} * v(t - \tau) + h_{r1} * h_{r2} * h_{r1} * v(t - 3\tau) + h_{r1}^{*2} * h_{r2}^{*2} * h_{r1} * v(t - 5\tau) + \dots \quad (2)$$

where  $\tau$  is the propagation time of waves in the line,  $h^{*n}$  means an  $n$ -times convolution of  $h$  by itself, and  $v$  is the voltage injected at bus 2. This voltage is a function of time and in this case can be considered as a step function.

Laplace transform of (2) outcomes in:

$$V_1(s) = H_{r1} V e^{-\tau s} + H_{r1} H_{r2} H_{r1} V e^{-3\tau s} + H_{r1}^2 H_{r2}^2 H_{r1} V e^{-5\tau s} + \dots \quad (3)$$

and it can be written in a compact form as:

$$V_1(s) = V H_{r1} e^{-s\tau} \sum_{n=0}^M (H_{r1} H_{r2} e^{-2s\tau})^n \quad (4)$$

Where  $M$  is the number of considered wave front arrivals and  $V$  is the Laplace transform of  $v$ .

Reflection and refraction coefficients of transmission line of Fig. 4 in frequency domain are:

$$H_{r1} = [sL_1 - (Zc - R_1)](sL_1 + Zc)^{-1}, \quad (5)$$

$$H_{r2} = (R_2 - Zc)(R_2 + Zc)^{-1}, \quad (6)$$

$$H_{t1} = 2(sL_1 + R_1)(sL_1 + Zc + R_1)^{-1}. \quad (7)$$

Equation (4) is a geometric series that converges to

$$V_1(s) = V H_{r1} e^{-s\tau} \frac{1 - (H_{r1} H_{r2})^M e^{-2Ms\tau}}{1 - H_{r1} H_{r2} e^{-2s\tau}}. \quad (8)$$

System of Fig. 4 is linear and can be represented by the following transfer function:

$$Tf(s) = \frac{V_1(s)}{V} = H_{r1} e^{-s\tau} \frac{1 - (H_{r1} H_{r2})^M e^{-2Ms\tau}}{1 - H_{r1} H_{r2} e^{-2s\tau}}. \quad (9)$$

The behavior of (9) with  $s = j\omega$  shows how the frequencies of an arbitrary input are filtered. By evaluating the modulus of (9), it is possible to identify a progression of higher peaks among little peaks. The higher peaks are independent of  $M$  and allow the passage of characteristics frequencies. To locate these peaks is enough to find the maximum modulus of the quotient part in (9). This modulus can be expressed at a specific frequency  $\omega$  as:

$$f(\omega) = \frac{1 + H_{r12}^{2M} - 2H_{r12}^M \cos(aM\omega + M\theta)}{1 + H_{r12}^2 - 2H_{r12} \cos(a\omega + \theta)}, \quad (10)$$

where:

$$H_{r12} = |H_{r1}(\omega) H_{r2}(\omega)|, \quad (11)$$

$$\theta = \angle(H_{r1}(\omega) H_{r2}(\omega)), \quad (12)$$

$$a = 2\tau. \quad (13)$$

Greatest peaks in (10) are spaced at characteristics frequencies given by:

$$\omega_c = \frac{2n\pi - \theta}{a}. \quad (14)$$

Then, the lowest characteristic frequency is found by substituting (12) and (13) in (14) and taking  $n = 0$ . This frequency expressed in Hertz, with  $\tau$  in seconds and  $\theta$  in radians is:

$$f_c = \frac{2\pi - \theta}{4\pi\tau}. \quad (15)$$

#### B. Relation between equation of spectrum and fault location

A faulted line can be studied with Fig. 4 as follows. In many cases the fault can be modeled as a resistance much lower than the characteristic impedance of the line. Assuming this, the faulted point can be well represented as bus 2 in Fig. 4 with  $R_2$  as the fault resistance and  $x$  as the fault distance. Then,  $H_{r2}$  is a negative real number and the angle given in (12) is  $\pi$  plus angle of  $H_{r1}$ . The pure-fault line can be represented as a step-function voltage source with all others sources turned off. Then the pure effect of the fault can be studied by setting  $v(t)$  in bus 2 [13]. In conclusion, bus 1 represents the feeding terminal with short circuit impedance composed by  $R_1$  and  $L_1$ . The characteristic impedance of the line is  $Zc$ ,  $R_2$  the fault resistance and  $x$  the fault distance.

If a fault was detected and its characteristic frequency was measured, equation (15) can be rearranged to estimate a fault distance as:

$$x = \frac{2\pi - \theta}{4\pi f_{cm}} v, \quad (16)$$

where  $f_{cm}$  is the measured characteristic frequency and  $v$  is the

wave propagation velocity calculated for  $f_{cm}$ . As faults can be considered as pure resistive and lower than  $Z_c$ ,  $H_{r2}$  is a real negative number. Then, two extreme conditions can be inferred. When impedance at bus 1 is a resistance lower than  $Z_c$ , the angle  $\theta$  is 0 and (16) is reduced to:

$$x = \frac{v}{2f_{cm}}. \quad (17)$$

If impedance at bus 1 is a resistance higher than  $Z_c$ ,  $\theta$  is  $\pi$  and (16) is reduced to

$$x = \frac{v}{4f_{cm}}. \quad (18)$$

When impedance at bus 1 is composed by an inductance,  $\theta$  lies between 0 and  $\pi$ . Thus is necessary to use general (16) to solve the fault location problem. Observe that when  $L_1$  tend to infinity,  $\theta$  is always  $\pi$  leading (18). It is important to note that the angle of a complex number always lies between 0 and  $\pi$ .

### C. General behavior of frequencies versus fault distances

If all inductances and resistances of the system represented in Fig. 4 were constant with frequency, the angle of (12) can be given as:

$$\theta = \pi - \tan^{-1} \left( \frac{\omega}{\frac{Z-R}{L}} \right) - \tan^{-1} \left( \frac{\omega}{\frac{Z+R}{L}} \right). \quad (19)$$

Considering Fig. 4, when a fault is near bus 1 the frequency is higher and (19) tend to  $\pi$  for a constant  $L_1$ . If  $L_1$  is small the angle approximate slower to  $\pi$  than if  $L_1$  is higher. The latter conclusions can be seen with the next example. Consider the transmission line of Fig. 4 with  $Z_c = 929 \Omega$ ,  $R_2 = 10 \Omega$ ,  $R_1 = 1.5 \Omega$  and a varying  $L_1$ . Fig. 5 shows the characteristic frequency as a function of fault distance  $x$  and the inductance at measurement point, with  $x$  varying from 1 to 30 km.

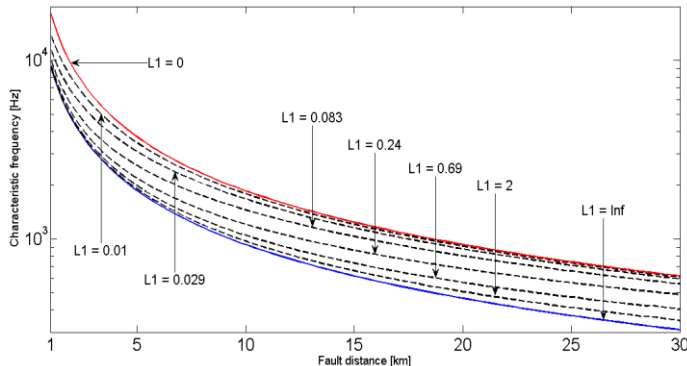


Fig. 5. Characteristic frequency as a function of fault distance and the inductance at measurement point (frequency axe is logarithmically scaled).

According with Fig. 5 and (16), the characteristic frequency is inversely proportional with  $x$ . But as  $\theta$  just vary with frequency, characteristic frequency approximate to one of extremes conditions only on determinates ranges of distances. For that reason the  $n_p$  factor in (1) cannot be considered as a

constant with frequency.

## IV. STUDIED CASES

In order to demonstrate the effectiveness of the developed equations, a typical Brazilian sub-transmission line was modeled using ATP. This line has a length of 30 km and a nominal voltage of 69 kV connecting the substation of Charquedas2 with Areal, in the state of Rio Grande do Sul. A schematic diagram of line and the fault model are defined in Fig. 6.

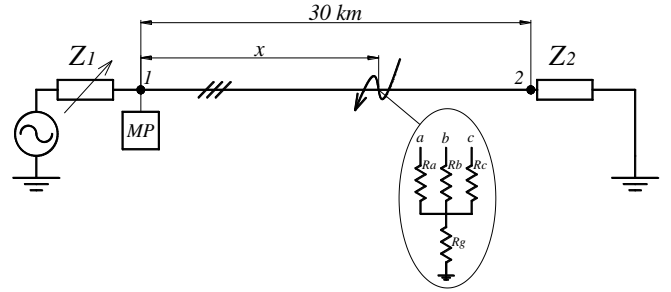


Fig. 6. Line electric diagram and fault model.

The model was considered with three different values of  $Z_1$  leading to three case studies. The First one has the originally specified value of  $Z_1$ ; the others two have the  $Z_1$  arbitrary modified in simulations for testing the effectiveness of (16). Values of  $Z_1$  are presented in Table I and simulated fault are showed in Table II.

TABLE I  
TEST SYSTEMS

Case	$R_0$ [ $\Omega$ ]	$L_0$ [H]	$R_+$ [ $\Omega$ ]	$L_+$ [H]
1	1.57	0.0156	1.41	0.02
2	3.15	0.042	2.82	0.03
3	3.15	0.08	2.82	0.058

$R_0$  and  $L_0$  are zero sequence parameters;  
 $R_+$  and  $L_+$  are positive and negative sequence parameters.

TABLE II  
SIMULATED FAULTS ON TEST SYSTEM

Fault Id.	Fault type	Dist. [km]	$R_a$ [ $\Omega$ ]	$R_b$ [ $\Omega$ ]	$R_c$ [ $\Omega$ ]	$R_g$ [ $\Omega$ ]
A	abc-g	4	0.2	0.2	0.2	0
B	c-g	7.3	-	-	10	10
C	ab-g	17	5	5	-	10
D	bc	23.6	-	6	10	-

Fault Id: Fault identification letter;

To adequately model the travelling waves, the line was modeled using J. Marti's frequency dependent model [18], considering a transposed line case.

### A. Proposed algorithm for fault location

In this section is proposed a series of steps that should be followed to perform the fault location by the fault characteristic frequency approach.

- 1) Fault detection and recording of faulted three phase voltages;
- 2) Clarke transformation to obtain the 0,  $\alpha$ , and  $\beta$  voltages;

- 3) DFT of  $\alpha$  or  $\beta$  voltages;
- 4) Find the measured characteristic frequency;
- 5) Calculation of  $\theta$  for the characteristic frequency;
- 6) Calculation of wave propagation velocity at the characteristic frequency;
- 7) Estimate the fault distance with (16).

Aforementioned steps need some clarifications: to perform fault detection there are many approaches in literature and practice. Commonly, all methods are based on definition of some threshold level to activate the recording. Here the Park's transformation approaches were used. It was proposed by [8] and an analysis of the method is found in [9]. Clarke transformation is a way to turn the three-phase voltages into three decoupled modal voltages called 0,  $\alpha$  and  $\beta$ . It was chosen because in cases of transposed lines, it matches with modal transformation and symmetrical components [15]. The DFT analysis was made with a Matlab algorithm proposed in [16]. For calculating angle  $\theta$ , the infinites series given by Carson were used [17].

### B. Results and analysis

Each faults showed in Table II were applied to each system case of Table I. In Table III the results are summarized, showing the measured characteristic frequency, the angle  $\theta$  and velocity  $v$  calculated with characteristic frequency, calculated fault distance and associated error. Analysis was made with  $\alpha$  mode of Clarke transformation except for the BC fault. These modes were chosen because they have less variation with frequency. Tests were carried out with a sampling frequency of 1 MHz and a spacing of 50 Hz between frequencies.

TABLE III  
RESULTS WITH SAMPLE FREQUENCY OF 1MHz

Mod	Fault Id.	Case	$f_{cm}$ [Hz]	$\theta$ [rad]	$v$ [km/s]	Dist. [km]	Error %
$\alpha$	A	1	20 400	2.822	297 250	4.01	0.03
		2	19 800	2.917	297 230	4.02	0.06
		3	19 200	3.019	297 210	4.02	0.06
$\alpha$	B	1	12 000	2.606	296 810	7.23	0.23
		2	10 800	2.733	296 710	7.76	1.53
		3	10 050	2.907	296 630	7.9	2.00
$\alpha$	C	1	5700	2.087	295 980	17.33	1.10
		2	5400	2.350	295 920	17.15	0.50
		3	4950	2.670	295 820	17.18	0.60
$\beta$	D	1	4350	1.897	295 770	23.70	0.33
		2	4050	2.176	295 700	23.86	0.86
		3	3600	2.537	295 580	24.47	2.90

Results presented in Table III are very accurate, even though were used much higher sample frequency than that usually used in common commercial equipment. For this reason, some tests were made with a commercial sampling frequency of 15 kHz. These results are showed in Table IV.

TABLE IV  
RESULTS WITH SAMPLE FREQUENCY OF 15 kHz

Mod	Fault Id.	Case	$f_{cm}$ [Hz]	$\theta$ [rad]	$v$ [km/s]	Dist. [km]	Error %
$\alpha$	C	1	5850	2.087	295980	16.89	0.36
		2	5422	2.350	295920	17.08	0.26
		3	4995	2.670	295820	17.03	0.10
$\beta$	D	1	4500	1.897	295770	22.94	2.20
		2	4200	2.176	295700	23.01	1.96
		3	3727	2.537	295580	23.64	0.13

In the last case it was not possible to locate faults that generate a characteristic frequency less than that limited by Nyquist theorem (7500 Hz in this case)

### V. CONCLUSIONS

A simplified analysis, factor  $n_p$  in (1) only considers extreme cases of  $Z_s$ . That means that imaginary part of  $Z_s$  is considered large or small or  $Z_s$  is considered as a real number. With former assumptions (1) can be used with an  $n_p$  equal to 4 or 2. When  $Z_s$  has intermediate values it is necessary to use another approach. To solve de problem, equation (16) were developed. This equation can perfectly take into account frequency dependence of line impedance,  $Z_s$  and fault impedance. Thereby, the proposed approach is general and can be adapted to many situations.

Equation (16) was developed for a single line case. Then, measurements in studied case have been decoupled with Clarke's transformation and voltages at  $\alpha$  or  $\beta$  modes were analyzed.  $\alpha$  mode was chosen because line parameters have less variation with frequency. However, for BC faults it was necessary to use  $\beta$  mode because  $\alpha$  have no information. Taking former considerations, errors on fault distance estimation were less than 1% in 60% of simulated cases and less than 3% on the rest for a sampling frequency of 1 MHz. Considering a commercial sampling frequency of 15 kHz, results are equal than with 1 MHz. Nonetheless, by limitations of Nyquist theorem, only faults located more than 15 km can be located.

Effects of voltage transformer were not studied in this work. It is well known that they have quite limited frequency characteristic that may make impossible to directly implement the proposed method. In that way, present work was developed principally to give a new insight of fault location based on high frequency components. Another side of the physics involved is shown that may contribute in futures works.

### VI. REFERENCES

- [1] T. Takagi, Y. Yamakoshi, M. Yamaura, R. Kondow, T. Matushima. "Development of a New Type Fault Locator Using the One-terminal Voltage and Current Data" *IEEE Trans. On Power Apparatus and Systems*, vol. 101, no. 8, pp. 2892-2898, Aug. 1982.
- [2] L. Eriksson, M. Saha, G. D. Rockefeller "An Accurate Fault Locator with Compensation for Apparent Reactance in the Fault Resistance Resulting from Remote-end Infeed" *IEEE Trans. on Power Apparatus and Systems*, vol. 104, no. 2, pp. 424-36, Feb. 1985.

- [3] R. H. Salim, K. C. O. Salim, A. S. Bretas "Further Improvements on Impedance-based Fault Location for Power Distribution Systems" *IET Generation, Transmission and Distribution*, vol. 5, pp. 467-478, 2011.
- [4] T. W. Stringfield, D. J. Marihat, R. F. Stevens. "Fault location methods for overhead lines" *IAEE Power Apparatus And Systems, Part III*, vol. 76, pp. 518-530, Apr. 1957.
- [5] M. M. Saha, J. Izykowski, E. Rosolowski. *Fault Location on Power Network*. New York: Springer-Verlag, 2010.
- [6] O. M. K. Kasun Nanayakkara, Athula. D. Rajapakse, Randy Wachal. "Fault Location of DC Line Faults in Conventional HVDC Systems with Segments of Cables and Overhead Lines Using Terminal Measurements" *IEEE Trans. Power Delivery*, vol. 27, pp. 279-288, Jan. 2012
- [7] Z. Q. Bo, G. Weller, M. A. Redfern. Accurate fault location technique for distribution system using fault-generated high-frequency transient voltage signals" in *Proc. 1999 IEE Generation, Transmission and Distribution*, Nottingham, v. 146, n. 1, p. 73-79.
- [8] F. V. Lopes, W. C. Santos, D. Fernandes, W. L. A. Neves, B. A. Souza "An Adaptive Fault Location Method for Smart Distribution and Transmission Grids" in *Proc. 2011 Innovative Smart Grid Technologies (ISGT Latin America)*.
- [9] R. G. Ferraz, L. U. Iurinic, A. D. Filomena, A. S. Bretas "Park's transformation analytical approach of transient signal analysis for power systems" In *Proc. IEEE 2012 North American Power Symposium*.
- [10] F. H. Magnago, A. ABUR, "Fault Location Using Wavelets", *IEEE Trans. Power Delivery*, vol. 13, no. 4, pp.1475-1480, Oct. 1998
- [11] Giovanni Miano, *Transmission lines and lumped circuits*, Academic Press, San Diego, USA, 2001, pp. 64-84.
- [12] G. W. Swift, "The spectra of fault-induced transients" *IEEE Transactions on Power Apparatus and Systems*, vol. 98, no. 3, pp. 940-947, May 1979.
- [13] A. Borghetti, M. Bosetti, C. A. Nucci, M. Paolone, A. Abur "Integrated Use of Time-Frequency Wavelet Decompositions for Fault Location in Distribution Networks: Theory and Experimental Validation", *IEEE Trans. On Power Delivery*, vol. 25, no. 4, Oct. 2010.
- [14] Lin-Yong Wu, Zheng-You He, Qing-Quan Qian "A New Single Ended Fault Location Technique Using Travelling Wave Natural Frequencies" In *Proc. IEEE 2009 Asia-Pacific Power and Energy Engineering Conference*.
- [15] H. W. Dommel, *ElectroMagnetic Transients Program. Reference Manual (EMTP Theory Book)*, Bonneville Power Administration, 1986.
- [16] V. K. Ingle, J. G. Proakis, *Digital Signal Processing using Matlab*, Stamford: Cengage Learning, 2011.
- [17] J. R. Carson "Wave Propagation in Overhead Wires with Ground Return" *Bell Syst. Tech. J.*, vol. 5, pp. 539-554, 1926.
- [18] J. MARTI, J. "Accurate Modeling of Frequency - Dependent Transmission Lines in Electromagnetic Transient Simulations", *IEEE Transactions on Power Apparatus and Systems*, vol.PAS- 101, No.1, pp.147-157, Jan. 1982.